

3D inverse dynamics in non-orthonormal segment coordinate system

R. Dumas · L. Chèze

Received: 22 June 2006 / Accepted: 23 December 2006
© International Federation for Medical and Biological Engineering 2007

Abstract The net joint forces and moments may be computed by several 3D inverse dynamic methods. To do so, an orthonormal segment coordinate system (SCS) is generally mandatory. However, the segment axes ought to be selected following anatomical, functional, and inertial requirements that are hardly compatible with orthogonal axes. An alternative method based on generalized coordinates allows computing inverse dynamics using directly a set of basic points and unitary vectors. A segment definition is put forward in order to follow all of the anatomical, functional, and inertial requirements and the inverse dynamics is performed in a non orthonormal segment coordinate system (NSCS). The NSCS seems a convenient definition in biomechanics as far as anatomical, functional and inertial axes are concerned, but providing that the 3D joint forces and moments are still computable. The inverse dynamic method in NSCS is applied to the gait of a knee valgus subject and compared to a classical inverse dynamic method. The inverse dynamic method in NSCS shows comparable results but implies further clinical interpretations.

Keywords 3D inverse dynamics · Joint forces and moments · Segment coordinate system · Generalized coordinates · Non orthonormal system

1 Introduction

Net joint forces and moments obtained from inverse dynamics are widely used in biomechanics, orthopaedics, and ergonomics. Four 3D inverse dynamic methods have been proposed in the literature either based on vectors and Euler angles [13, 33, 43], homogenous matrices [15], wrenches and quaternions [18] or generalized coordinates [39, 40].

In the first three methods, an orthonormal segment coordinate system (SCS) is mandatory. Several proposals have been reported for SCS [1, 6, 46], trying to follow requirements hardly compatible with orthogonal axes: the SCS ought to be consistent with the anatomical axis (i.e., “body link” from proximal to distal joint centre [7, 14]); the SCS ought to be consistent with the estimated in vivo functional axis of the joint [11, 38, 5, 44] in order to construct a reliable joint coordinate system (JCS) [21, 46] and; the SCS ought to be consistent with the inertial axes (i.e., compatible with the estimation of inertial parameters from literature [32, 35]). The sensitivity of 3D kinematics and 3D inverse dynamics to joint centre position, functional axis orientation and inertial parameter estimation is well established [4, 24, 30, 31, 34, 42]. For this reason, the segment axes should not be selected with prioritizing one of the anatomical, functional or inertial axes in order to enforce orthogonality.

In this way, the fourth inverse dynamics method proposed in the literature [39, 40] is based on generalized coordinates where no SCS is required: the position and orientation of the segment can simply be defined by a set of basic points and unitary vectors. The feasibility of inverse dynamics using generalized coordinates was demonstrated by Silva and Ambrosio

R. Dumas · L. Chèze
Université de Lyon, Lyon 69003, France

R. Dumas (✉) · L. Chèze
Laboratoire de Biomécanique et Modélisation Humaine
(UCBL/INRETS), Université Lyon 1, Bât. Oméga,
Bd du 11 Novembre 1918, Villeurbanne 69622, France
e-mail: raphael.dumas@univ-lyon1.fr

[39]. However, these authors reported a very specific human body model consisting of 33 rigid bodies and 32 joints for 16 segments. Typically, one rigid body is associated to one degree-of-freedom (following the Hartenberg–Denavit description [23]). For these rigid bodies, the generalized coordinates were two basic points and one unitary vector chosen orthogonal to the basic point line (even though generalized coordinates do not require orthogonality). Moreover, only the moments about the pre-determined rotation axes (along with the unitary vectors or the basic point line) were computed by inverse dynamics rather than the 3D joint forces and moments as in all other methods. Actually, these moments were the Lagrange multipliers related to additional rotational driver constraints about a chosen axis. Furthermore, very unusual inertial parameters had to be defined for each rigid body. The advantages of the generalized coordinates for the definition of such a kinematical model have been reported [25, 39]. The use of a kinematical model is mandatory in forward dynamics but may be avoided in inverse dynamics when computing the Newton–Euler equations recursively. This recursive computation is more commonly reported [4, 13, 15, 18, 24, 31, 34, 42, 43]. In this way, the advantages of the generalized coordinates for the definition of one single segment in recursive inverse dynamic computation are not well established.

Therefore, the objectives of this paper are (1) to propose a segment definition based on the generalized coordinates that can be compatible with all of the anatomical, functional, and inertial axes, and (2) to develop an inverse dynamic method in non orthonormal SCS (NSCS) that can compute the same 3D joint forces and moments as in the other reported methods. The method is presented for the right lower limb and compared with the classical inverse dynamic method (based on Euler angles), on the gait of a knee valgus subject.

2 Methods

2.1 Non orthonormal segment coordinate system

2.1.1 Generalized coordinates

The thigh, shank and foot segments are denoted, respectively, $i = 3, 2, 1$. The generalized coordinates proposed for these segments (Fig. 1) consist of two position vectors of the proximal endpoint P_i and the distal endpoint D_i and of two unitary direction vectors (\mathbf{u}_i and \mathbf{w}_i):

$$\mathbf{Q}_i = \begin{bmatrix} \mathbf{u}_i \\ \mathbf{r}_{P_i} \\ \mathbf{r}_{D_i} \\ \mathbf{w}_i \end{bmatrix}. \quad (1)$$

All vectors are expressed in an inertial coordinate system (ICS) and can be computed from commonly used anatomical landmarks [1, 6, 13, 43, 46] and from joint centres and functional axes estimated from in vivo motion data [11, 20, 22, 36, 38, 5, 44]. For the thigh, the endpoint P_3 is the hip joint centre (HJC) and the endpoint D_3 is the knee joint centre (KJC). The vector \mathbf{u}_3 is normal to the plane formed by HJC, lateral and medial femoral epicondyles (MFE and MFE), pointing anteriorly. The vector \mathbf{w}_3 is the estimated in vivo functional flexion–extension axis of the knee. Alternatively, \mathbf{w}_3 can be the vector from MFE to LFE. For the shank, the endpoint P_2 is the KJC and the endpoint D_2 is the ankle joint centre (AJC). The vector \mathbf{u}_2 is normal to the plane formed by fibula head (FH),

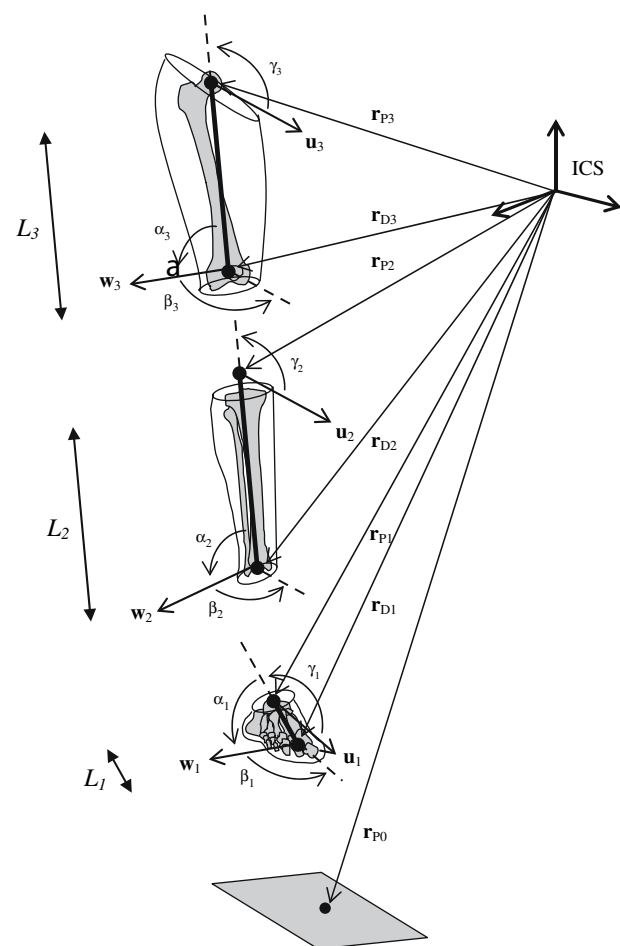


Fig. 1 Non orthonormal segment coordinate system (NSCS) of thigh, shank and foot: generalized coordinates and rigid body constraints

lateral and medial maleoli (LM and MM), pointing anteriorly. The vector \mathbf{w}_2 is the estimated in vivo functional flexion–extension axis of the ankle. Alternatively, \mathbf{w}_2 can be the vector from MM to LM. For the foot, the endpoint P_1 is the AJC and the endpoint D_1 is the middle of first and fifth metatarsal (M1 and M5). The vector \mathbf{u}_1 is from calcaneus (CAL) to the middle of M1 and M5. The vector \mathbf{w}_1 is from M1 to M5.

The generalized coordinates yield 4×3 parameters ($\mathbf{u}_i, \mathbf{r}_{P_i}, \mathbf{r}_{D_i}$ and \mathbf{w}_i) for the six degrees of freedom of the segment. Thus, six rigid body constraints (Fig. 1) are introduced [25]:

$$\begin{cases} \mathbf{u}_i^2 - 1 = 0 \\ \mathbf{u}_i(\mathbf{r}_{P_i} - \mathbf{r}_{D_i}) - L_i \cos \gamma_i = 0 \\ \mathbf{u}_i \mathbf{w}_i - \cos \beta_i = 0 \\ (\mathbf{r}_{P_i} - \mathbf{r}_{D_i})^2 - L_i^2 = 0 \\ (\mathbf{r}_{P_i} - \mathbf{r}_{D_i}) \mathbf{w}_i - L_i \cos \alpha_i = 0 \\ \mathbf{w}_i^2 - 1 = 0 \end{cases} \quad (2)$$

with $0 \leq \alpha_i \leq \pi$, $0 \leq \beta_i \leq \pi$ and $0 \leq \gamma_i \leq \pi$.

2.1.2 Segment coordinate system

The proposed generalized coordinates allow defining a NSCS ($P_i, \mathbf{u}_i, (\mathbf{r}_{P_i} - \mathbf{r}_{D_i}), \mathbf{w}_i$). The vector \mathbf{u}_i is normal to the frontal plane of the segment and is associated to an inertial axis. The vector $(\mathbf{r}_{P_i} - \mathbf{r}_{D_i})$ corresponds to the anatomical axis of the segment. The norm of the anatomical axis $L_i = \|\mathbf{r}_{P_i} - \mathbf{r}_{D_i}\|$ corresponds to the segment length. The vector \mathbf{w}_i corresponds to the esti-

estimated in vivo functional axis. For example, concerning the knee, the first rotation axis \mathbf{e}_1 is fixed to the thigh segment and coincident with \mathbf{w}_3 . The rotation is extension (positive) or flexion (negative). The third rotation axis \mathbf{e}_3 is fixed to the shank segment and coincident with $(\mathbf{r}_{P_i} - \mathbf{r}_{D_i})$. The rotation is internal rotation (positive) or external rotation (negative). The second rotation axis \mathbf{e}_2 is floating and coincident with the common axis perpendicular to \mathbf{e}_1 and \mathbf{e}_3 . The rotation is adduction (positive) or abduction (negative).

2.2 Inverse dynamics in a non orthonormal segment coordinate system

2.2.1 Equation of motion

The equation of motion of the segment ($i = 1, 2, 3$) is written in the ICS with Lagrange multipliers λ_i :

$$\begin{aligned} [\mathbf{G}_i] \ddot{\mathbf{Q}}_i + [\mathbf{K}_i]^T \lambda_i \\ = [\mathbf{N}_i^{C_i}]^T m_i \mathbf{g} + [\mathbf{N}_i^{P_i}]^T (\mathbf{F}_i - \mathbf{F}_{i-1}) \\ + [\mathbf{N}_i^*]^T (\mathbf{M}_i - \mathbf{M}_{i-1} + (\mathbf{r}_{P_{i-1}} - \mathbf{r}_{P_i}) \times (-\mathbf{F}_{i-1})) \end{aligned} \quad (3)$$

where

$$\ddot{\mathbf{Q}}_i = \begin{bmatrix} \ddot{\mathbf{u}}_i \\ \ddot{\mathbf{r}}_{P_i} \\ \ddot{\mathbf{r}}_{D_i} \\ \ddot{\mathbf{w}}_i \end{bmatrix} \quad (4)$$

is the generalized acceleration and where \mathbf{K}_i is the Jacobian matrix of the rigid body constraints (Eq. 2):

$$[\mathbf{K}_i]^T = \begin{bmatrix} 2\mathbf{u}_i & (\mathbf{r}_{P_i} - \mathbf{r}_{D_i}) & \mathbf{w}_i & \mathbf{0}_{3 \times 1} & \mathbf{0}_{3 \times 1} & \mathbf{0}_{3 \times 1} \\ \mathbf{0}_{3 \times 1} & \mathbf{u}_i & \mathbf{0}_{3 \times 1} & 2(\mathbf{r}_{P_i} - \mathbf{r}_{D_i}) & \mathbf{w}_i & \mathbf{0}_{3 \times 1} \\ \mathbf{0}_{3 \times 1} & -\mathbf{u}_i & \mathbf{0}_{3 \times 1} & -2(\mathbf{r}_{P_i} - \mathbf{r}_{D_i}) & -\mathbf{w}_i & \mathbf{0}_{3 \times 1} \\ \mathbf{0}_{3 \times 1} & \mathbf{0}_{3 \times 1} & \mathbf{u}_i & \mathbf{0}_{3 \times 1} & (\mathbf{r}_{P_i} - \mathbf{r}_{D_i}) & 2\mathbf{w}_i \end{bmatrix}. \quad (5)$$

ated functional axis of the segment. All the inverse dynamics is computed in these NSCS (see “[Inverse dynamics in a non segment coordinate system](#)”).

2.1.3 Joint coordinate system

Moreover, the proposed generalized coordinates allow constructing the JCS [21, 46] on the basis of the

All other terms are defined hereafter.

2.2.2 Generalized mass matrix

In the equation of motion, the generalized mass matrix is [25]:

$$[\mathbf{G}_i] = \begin{bmatrix} J_{i11} \mathbf{E}_{3 \times 3} & (m_i n_i^{C_i} + J_{i12}) \mathbf{E}_{3 \times 3} & -J_{i12} \mathbf{E}_{3 \times 3} & J_{i13} \mathbf{E}_{3 \times 3} \\ (m_i + 2m_i n_i^{C_i} + J_{i22}) \mathbf{E}_{3 \times 3} & (-m_i n_i^{C_i} - J_{i22}) \mathbf{E}_{3 \times 3} & J_{i22} \mathbf{E}_{3 \times 3} & (m_i n_i^{C_i} + J_{i23}) \mathbf{E}_{3 \times 3} \\ -J_{i22} \mathbf{E}_{3 \times 3} & J_{i22} \mathbf{E}_{3 \times 3} & -J_{i23} \mathbf{E}_{3 \times 3} & J_{i33} \mathbf{E}_{3 \times 3} \\ \text{symmetric} & & & \end{bmatrix} \quad (6)$$

where m_i is the segment mass, $\mathbf{n}_i^{C_i}$ are the coordinates of the centre of mass C_i expressed in the NSCS of segment i , \mathbf{J}_i is the pseudo inertia tensor expressed at the proximal endpoint P_i and in the NSCS of segment i , and where $\mathbf{E}_{3 \times 3}$ is the identity matrix.

In the NSCS, $\mathbf{n}_i^{C_i}$ and \mathbf{J}_i are computed on the basis of classical regression estimations using the segment length L_i [8, 28, 14, 16]. In these estimations, the position of the centre of mass \mathbf{c}_i^s is given with respect to the proximal endpoint P_i and the principal inertia tensor \mathbf{I}_i^s is given at the centre of mass C_i . Both are expressed in a SCS consistent with the frontal, sagittal and transverse planes. The \mathbf{u}_i axis has been constructed so that it is normal to the frontal plane of the segment. Thus, \mathbf{u}_i is directly consistent with the inertial parameter estimation. The non-unitary rotation matrix from the NSCS to the SCS consistent with the inertial parameter estimation is:

$$[\mathbf{B}_i^s] = \begin{bmatrix} 1 & L_i \cos \gamma_i & \frac{\cos \beta_i}{\sin \gamma_i} \\ 0 & L_i \sin \gamma_i & \frac{\cos \alpha_i - \cos \beta_i \cos \gamma_i}{\sin \gamma_i} \\ 0 & 0 & \sqrt{1 - (\cos \beta_i)^2 - \left(\frac{\cos \alpha_i - \cos \beta_i \cos \gamma_i}{\sin \gamma_i} \right)^2} \end{bmatrix}. \quad (7)$$

Therefore, the coordinates of the centre of mass in the NSCS is:

$$\mathbf{n}_i^{C_i} = \begin{bmatrix} n_{i1}^{C_i} \\ n_{i2}^{C_i} \\ n_{i3}^{C_i} \end{bmatrix} = [\mathbf{B}_i^s]^{-1} \mathbf{c}_i^s. \quad (8)$$

As well, the pseudo inertia tensor in the NSCS and at the proximal endpoint P_i (i.e., using Huygens theorem) is:

$$[\mathbf{J}_i] = [\mathbf{B}_i^s]^{-1} \left[[\mathbf{I}_i^s] + m_i \left((\mathbf{c}_i^s)^T \mathbf{c}_i^s \mathbf{E}_{3 \times 3} - \mathbf{c}_i^s (\mathbf{c}_i^s)^T \right) \right] \cdot ([\mathbf{B}_i^s]^{-1})^T. \quad (9)$$

2.2.3 Generalized forces and moments

In the equation of motion (Eq. 3), the generalized forces are obtained with interpolation matrices \mathbf{N}_i depending on the points of application [25]. For a concentrate force, as the segment weight $m_i \mathbf{g}$ applied on the segment at the centre of mass C_i , the interpolation matrix is:

$$[\mathbf{N}_i^{C_i}]^T = \begin{bmatrix} n_{i1}^{C_i} \mathbf{E}_{3 \times 3} \\ (1 + n_{i2}^{C_i}) \mathbf{E}_{3 \times 3} \\ -n_{i2}^{C_i} \mathbf{E}_{3 \times 3} \\ n_{i3}^{C_i} \mathbf{E}_{3 \times 3} \end{bmatrix}. \quad (10)$$

For a wrench, such as the distal force and moment expressed at D_i , a transformation is first proposed in order to consider the resultant action at the proximal endpoint P_i [18]. Also, the action–reaction principle in the ICS directly gives $-\mathbf{F}_{i-1}$ and $-\mathbf{M}_{i-1}$ expressed at $P_{i-1} = D_i$. For the foot ($i = 1$), the distal force and moment are $-\mathbf{F}_0$ and $-\mathbf{M}_0$, opposite of the ground reaction force and moment (applied on the force platform) expressed at the centre of pressure P_0 (see Fig. 1).

For the proximal and distal forces, \mathbf{F}_i and $-\mathbf{F}_{i-1}$, both considered at the proximal endpoint P_i , the same interpolation matrix is:

$$[\mathbf{N}_i^{P_i}]^T = \begin{bmatrix} \mathbf{0}_{3 \times 3} \\ \mathbf{E}_{3 \times 3} \\ \mathbf{0}_{3 \times 3} \\ \mathbf{0}_{3 \times 3} \end{bmatrix}. \quad (11)$$

For the proximal and distal moments both considered at the proximal endpoint P_i , \mathbf{M}_i and $-\mathbf{M}_{i-1} + (\mathbf{r}_{P_{i-1}} - \mathbf{r}_{P_i}) \times (-\mathbf{F}_{i-1})$ (due to the wrench transformation), a same pseudo-interpolation matrix \mathbf{N}_i^* is proposed, depending on the segment axes $(\mathbf{u}_i, \mathbf{r}_{P_i} - \mathbf{r}_{D_i}, \mathbf{w}_i)$:

$$[\mathbf{N}_i^*]^T = \begin{bmatrix} \mathbf{0}_{3 \times 1} & (\mathbf{r}_{P_i} - \mathbf{r}_{D_i}) & \mathbf{0}_{3 \times 1} \\ -\mathbf{u}_i & -(\mathbf{r}_{P_i} - \mathbf{r}_{D_i}) & -\mathbf{w}_i \\ \mathbf{0}_{3 \times 1} & \mathbf{0}_{3 \times 1} & \mathbf{w}_i \\ \mathbf{u}_i & \mathbf{0}_{3 \times 1} & \mathbf{0}_{3 \times 1} \end{bmatrix} [\mathbf{B}_i^*]^{-1} \quad (12)$$

where

$$[\mathbf{B}_i^*] = [\mathbf{w}_i \times \mathbf{u}_i \quad \mathbf{u}_i \times (\mathbf{r}_{P_i} - \mathbf{r}_{D_i}) \quad -(\mathbf{r}_{P_i} - \mathbf{r}_{D_i}) \times \mathbf{w}_i]. \quad (13)$$

Details can be found in [Appendix](#).

2.2.4 Inverse dynamics

Considering recursively each segment ($i = 1, 2, 3$), the 12 unknowns in the equation of motion (Eq. 3) are the proximal net joint force and moment 3D vectors (\mathbf{F}_i and \mathbf{M}_i) and the Lagrange multipliers vector λ_i (related to the six rigid body constraints). These unknowns are computed by inverse dynamics:

$$\begin{bmatrix} \mathbf{F}_i \\ \mathbf{M}_i \\ \lambda_i \end{bmatrix} = \begin{bmatrix} [\mathbf{N}_i^{P_i}]^T & [\mathbf{N}_i^*]^T & -[\mathbf{K}_i]^T \end{bmatrix}^{-1} \cdot \left([\mathbf{G}_i] \ddot{\mathbf{Q}}_i - [\mathbf{N}_i^{C_i}]^T m_i \mathbf{g} - [\mathbf{N}_i^{P_i}]^T (-\mathbf{F}_{i-1}) - [\mathbf{N}_i^*]^T \cdot (-\mathbf{M}_{i-1} + (\mathbf{r}_{P_{i-1}} - \mathbf{r}_{P_i}) \times (-\mathbf{F}_{i-1})) \right). \quad (14)$$

In this equation (Eq. 14), the matrices \mathbf{G}_i , $\mathbf{N}_i^{C_i^T}$ and $\mathbf{N}_i^{P_i^T}$ are constant.

2.3 Application

The gait at comfortable speed of a subject (23 years old, 1.75 m, 80 kg) with a 15° knee valgus is recorded at 100 Hz with motion analysis system (Santa Rosa, USA) and AMTI force platform (Watertown, USA). The vectors \mathbf{u}_i , \mathbf{r}_{P_i} , \mathbf{r}_{D_i} and \mathbf{w}_i are computed from the trajectories of markers placed on appropriate anatomical landmarks (see “Generalized coordinates”). These trajectories are expressed in an ICS with y -axis vertical and x -axis along with the walking direction [45], and are previously filtered (fourth-order Butterworth, 6 Hz cutoff frequency) and solidified [9]. More specifically, P_3 is the HJC determined functionally during a circumduction movement [10]. P_2 and \mathbf{w}_3 , as well as P_1 and \mathbf{w}_2 , are the centroids and mean directions of the helical axes determined functionally [11] (respectively, between thigh and shank segments and shank and foot segments) during a squat movement. The body segment inertial parameters (m_i , \mathbf{c}_i^s and \mathbf{I}_i^s) are estimated by regression using the segment length L_i [16]. The joint forces and moments are computed by the proposed method, normalized [29], and compared to the results of inverse dynamics by a classical method based on vectors and Euler angles [2, 3, 13, 19, 26, 43]. The Euler angles represent the attitude of the orthonormal SCS (see “Generalized mass matrix”) with a body zyx -sequence [45]. The so-called “flexion–extension” moments are expressed first about the z -axis of the ICS, and then about the w -axis of the proximal NSCS or the z -axis of the proximal SCS.

3 Results

The angles involved in the rigid body constraints of the foot segment (deduced from anatomical landmarks) are $\alpha_1 = 82^\circ$, $\beta_1 = 107^\circ$, $\gamma_1 = 167^\circ$. The angles for the shank and thigh segments (deduced from the functional axis, the subject performing the squat movement with the knee going medially) are $\alpha_2 = 69^\circ$, $\beta_2 = 67^\circ$, $\gamma_2 = 87^\circ$ and $\alpha_3 = 65^\circ$, $\beta_3 = 76^\circ$, $\gamma_3 = 89^\circ$.

The knee “flexion–extension” moment obtained by the present method and the classical inverse dynamic method (based on vectors and Euler angles) is presented in Fig. 2, about the z -axis of the ICS and about either the w -axis of the proximal NSCS or the z -axis of the proximal SCS.

4 Discussion

Using generalized coordinates, the position and orientation of the segment are simply described by a set of basic points and unitary vectors. This description is convenient for motion analysis as far as joint centres and functional axes are essential in 3D kinematics. That is why the proposed segment definition deals with both anatomical axis ($\mathbf{r}_{P_i} - \mathbf{r}_{D_i}$) and estimated functional axis \mathbf{w}_i . These axes are based on in vivo estimation from motion data [11, 20, 22, 36, 38, 5, 44] and this seems particularly appropriate for the construction of the JCS. Additionally, a third axis \mathbf{u}_i is proposed based on commonly used anatomical landmarks [1, 6, 13, 43, 46]. This is the only axis consistent with the

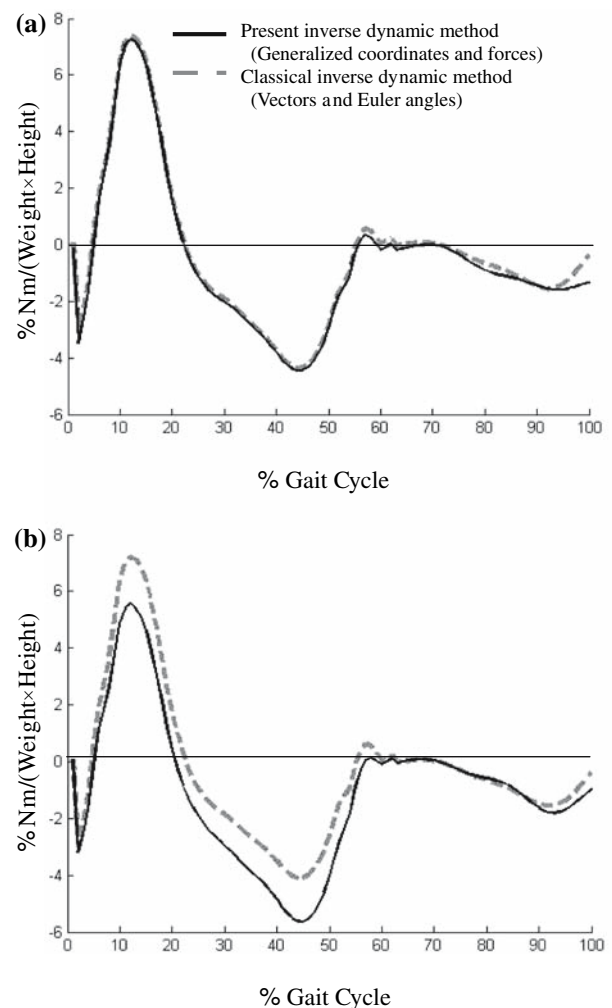


Fig. 2 Knee moment obtained by the present method (based on generalized coordinates and forces) and by the classical inverse dynamic method (based on vectors and Euler angles): **a** Flexion–extension moment about the z -axis of the ICS. **b** Flexion–extension moment about the w -axis of the proximal NSCS (for the present method) and about the z -axis of the proximal SCS (for the classical method)

frontal, sagittal and transverse plane of the segment according to the definition of Cappozzo et al. [6]. Consequently, \mathbf{u}_i is the only axis consistent with the inertial parameter estimations that commonly refer to these segment planes [8, 12, 28, 14, 47]. For the estimation of inertial parameters, the segment length L_i can be directly obtained from the norm of the anatomical axis $(\mathbf{r}_{P_i} - \mathbf{r}_{D_i})$. If, as in classical regressions [8, 28, 14], the position of the centre of mass is assumed to be aligned with the joint centres with a ratio r of the segment length, the coordinates of the centre of mass

in the NSCS are directly $\mathbf{n}_i^{C_i} = \begin{bmatrix} 0 \\ -r \\ 0 \end{bmatrix}$. That is why the

proposed segment definition seems to represent a convenient way to implement the data required for both 3D kinematics and inverse dynamics, as far as the anatomical, functional, and inertial axes are concerned.

However, these anatomical, functional, and inertial axes cannot stand for orthogonal axes and can hardly be compatible with 3D inverse dynamics when using methods based on Euler angles, homogenous matrices or quaternions [13, 15, 18, 33, 43]. On the opposite, the proposed inverse dynamic method allows computing the 3D joint forces and moments in the NSCS $(P_i, \mathbf{u}_i, (\mathbf{r}_{P_i} - \mathbf{r}_{D_i}), \mathbf{w}_i)$. Matrices of large dimension are involved but many are constant. Also, the Lagrange multipliers λ_i are supplementary unknowns but they are useful in order to monitor the rigid body constraints. As a recursive computation is performed (without considering a kinematical model), no constraints are introduced in order to take into account that the distal end of one segment D_i is the same as the proximal end of the adjacent segment P_{i+1} . However, this ensures that the action–reaction principle can be adequately applied at the same point.

The use of alternative methods to the Euler angles is a topical debate in biomechanics [27]. The Euler angles are required for the joint attitude (i.e., within the JCS) but may be avoided for the segment attitude because the Euler angles suffer from discontinuities and singularities [41] that may bias the inverse dynamic computation. In the same way as homogenous matrices and quaternions, the proposed method has the advantage of a singularity-free computation of the kinematics. Additionally, the only kinematics to derive is the generalized acceleration $\dot{\mathbf{Q}}_i$. On a subject with knee valgus, the comparison of the proposed method with the classical inverse dynamic method (based on vectors and Euler angles) demonstrates that the computation is reliable (similar results in the ICS), but allows further clinical interpretations (different results in SCS or NSCS). Actually, the proposed method has the

advantage of a segment definition taking into account all of the anatomical, functional, and inertial axes. Therefore, the joint forces and moments can be directly projected on the functional axis [37] and the JCS definition is also directly based on this functional axis.

Moreover, the comparison of four inverse dynamic methods (based on vectors and Euler angles, on homogenous matrices, on wrenches and quaternions, and on generalized coordinates and forces) during gait demonstrated almost similar patterns and amplitudes although different curves and different sensitivity to noise [17]. Therefore, the alternatives in 3D inverse dynamic methods should be better investigated, especially when the joint forces and moments are to be used for muscular models.

5 Conclusion

A segment definition is put forward in order to follow all of the anatomical, functional, and inertial requirements. Based on generalized coordinates and forces, the inverse dynamics is performed in a non orthonormal segment coordinate system (NSCS). The NSCS seems a convenient definition in biomechanics, as far as the non orthogonal joint coordinate system (JCS) is already accepted and as the functional axes of the joints become more and more investigated.

Acknowledgments The authors would like to thank Lionel Frossard, from University Claude Bernard Lyon1, for sharing his experience in rigid body dynamics using generalized coordinates.

6 Appendix

The interpolation matrix allows computing the position of a point in the ICS, knowing its coordinates in the NSCS $(P_i, \mathbf{u}_i, (\mathbf{r}_{P_i} - \mathbf{r}_{D_i}), \mathbf{w}_i)$ and the generalized coordinates of the segment. For example, the position vector of the centre of mass \mathbf{r}_{C_i} in the ICS can be expressed:

$$\mathbf{r}_{C_i} - \mathbf{r}_{P_i} = n_{i1}^{C_i} \mathbf{u}_i + n_{i2}^{C_i} (\mathbf{r}_{P_i} - \mathbf{r}_{D_i}) + n_{i3}^{C_i} \mathbf{w}_i. \quad (15)$$

This expression (Eq. 15) is written in matrix form:

$$\mathbf{r}_{C_i} = \underbrace{\begin{bmatrix} n_{i1}^{C_i} \mathbf{E}_{3 \times 3} & (1 + n_{i2}^{C_i}) \mathbf{E}_{3 \times 3} & -n_{i2}^{C_i} \mathbf{E}_{3 \times 3} & n_{i3}^{C_i} \mathbf{E}_{3 \times 3} \end{bmatrix}}_{[\mathbf{N}_i^{C_i}]} \cdot \begin{bmatrix} \mathbf{u}_i \\ \mathbf{r}_{P_i} \\ \mathbf{r}_{D_i} \\ \mathbf{w}_i \end{bmatrix}. \quad (16)$$

Four points, P_i , D_i , U_i and W_i , have remarkable coordinates in the NSCS (for $i = 1, 2$ and 3):

$$\mathbf{n}_i^{P_i} = \begin{bmatrix} 0 \\ 0 \\ 0 \end{bmatrix}, \quad \mathbf{n}_i^{D_i} = \begin{bmatrix} 0 \\ -1 \\ 0 \end{bmatrix},$$

$$\mathbf{n}_i^{U_i} = \begin{bmatrix} 1 \\ 0 \\ 0 \end{bmatrix} \text{ and } \mathbf{n}_i^{W_i} = \begin{bmatrix} 0 \\ 0 \\ 1 \end{bmatrix}.$$

The corresponding remarkable interpolation matrices are:

$$[\mathbf{N}_i^{P_i}]^T = \begin{bmatrix} \mathbf{0}_{3 \times 3} \\ \mathbf{E}_{3 \times 3} \\ \mathbf{0}_{3 \times 3} \\ \mathbf{0}_{3 \times 3} \end{bmatrix}, \quad [\mathbf{N}_i^{D_i}]^T = \begin{bmatrix} \mathbf{0}_{3 \times 3} \\ \mathbf{0}_{3 \times 3} \\ \mathbf{E}_{3 \times 3} \\ \mathbf{0}_{3 \times 3} \end{bmatrix},$$

$$[\mathbf{N}_i^{U_i}]^T = \begin{bmatrix} \mathbf{E}_{3 \times 3} \\ \mathbf{0}_{3 \times 3} \\ \mathbf{0}_{3 \times 3} \\ \mathbf{0}_{3 \times 3} \end{bmatrix} \text{ and } [\mathbf{N}_i^{W_i}]^T = \begin{bmatrix} \mathbf{0}_{3 \times 3} \\ \mathbf{0}_{3 \times 3} \\ \mathbf{0}_{3 \times 3} \\ \mathbf{E}_{3 \times 3} \end{bmatrix}.$$

These interpolation matrices can be used to compute the generalized forces applied at these points. Concerning moments, the generalized moments cannot be computed with interpolation matrices [25]. Moments have first to be replaced by couple of opposite forces.

The moment \mathbf{M} at proximal point P_i can be replaced by three forces about the three axes ($\mathbf{u}_i, \mathbf{r}_{P_i} - \mathbf{r}_{D_i}, \mathbf{w}_i$) and applied at the three points U_i , W_i and D_i :

$$\mathbf{M} = \mathbf{w}_i \times (f_1 \mathbf{u}_i) + \mathbf{u}_i \times (f_2 (\mathbf{r}_{P_i} - \mathbf{r}_{D_i})) + (- (\mathbf{r}_{P_i} - \mathbf{r}_{D_i})) \times (f_3 \mathbf{w}_i). \quad (17)$$

This expression (Eq. 17) is written in matrix form:

$$\mathbf{M} = \underbrace{\begin{bmatrix} \mathbf{w}_i \times \mathbf{u}_i & \mathbf{u}_i \times (\mathbf{r}_{P_i} - \mathbf{r}_{D_i}) & -(\mathbf{r}_{P_i} - \mathbf{r}_{D_i}) \times \mathbf{w}_i \end{bmatrix}}_{[\mathbf{B}_i]} \begin{bmatrix} f_1 \\ f_2 \\ f_3 \end{bmatrix}. \quad (18)$$

Three opposite forces are applied at endpoint P_i in order to maintain equilibrium. Thus, six concentrated forces are required to represent the moment and the generalized moment is:

$$[\mathbf{N}_i^*]^T \mathbf{M} = [\mathbf{N}_i^{W_i}]^T (f_1 \mathbf{u}_i) + [\mathbf{N}_i^{U_i}]^T (f_2 (\mathbf{r}_{P_i} - \mathbf{r}_{D_i})) + [\mathbf{N}_i^{D_i}]^T (f_3 \mathbf{w}_i) + [\mathbf{N}_i^{P_i}]^T (-f_1 \mathbf{u}_i - f_2 (\mathbf{r}_{P_i} - \mathbf{r}_{D_i}) - f_3 \mathbf{w}_i). \quad (19)$$

Therefore, the pseudo-interpolation matrix is (Eq. 12):

$$[\mathbf{N}_i^*]^T = \begin{bmatrix} \mathbf{0}_{3 \times 1} & (\mathbf{r}_{P_i} - \mathbf{r}_{D_i}) & \mathbf{0}_{3 \times 1} \\ -\mathbf{u}_i & -(\mathbf{r}_{P_i} - \mathbf{r}_{D_i}) & -\mathbf{w}_i \\ \mathbf{0}_{3 \times 1} & \mathbf{0}_{3 \times 1} & \mathbf{w}_i \\ \mathbf{u}_i & \mathbf{0}_{3 \times 1} & \mathbf{0}_{3 \times 1} \end{bmatrix} [\mathbf{B}_i^*]^{-1}.$$

References

- Allard P, Stokes IAF, Blanchi J (1995) Three-dimensional analysis of human movement. Human Kinetics, Champaign
- Allard P, Lachance R, Aissaoui R, Duhaime M (1996) Simultaneous bilateral 3-D able-bodied gait. Hum Mov Sci 15:327–346
- Apkarian J, Naumann S, Cairns B (1989) A three-dimensional kinematic and dynamic model of the lower limb. J Biomech 22:143–155
- Besier TF, Sturnieks DL, Alderson JA, Lloyd DG (2003) Repeatability of gait data using a functional hip joint centre and a mean helical knee axis. J Biomech 36:1159–1168
- van den Bogert AJ, Smith GD, Nigg BM (1994) In vivo determination of the anatomical axes of the ankle joint complex: an optimization approach. J Biomech 27:1477–1488
- Cappozzo A, Catani F, Croce UD, Leardini A (1995) Position and orientation in space of bones during movement: anatomical frame definition and determination. Clin Biomech 10:171–178
- Chaffin DB, Anderson GBJ (1991) Occupational biomechanics. Wiley, New York
- Chandler RF, Clauser CE, McConville JT, Reynolds HM, Young JW (1975) Investigation of inertial properties of the human body. Technical report AMRL-74–137. Aerospace Medical Research Laboratory, Wright-Patterson Air Force Base, Dayton
- Chèze L, Fregly BJ, Dimnet J (1995) A solidification procedure to facilitate kinematic analyses based on video system data. J Biomech 28:879–884
- Chèze L, Gutierrez C, San-Marcelino R, Dimnet J (1996) Biomechanics of the upper limb using robotic techniques. Hum Mov Sci 15:477–496
- Chèze L, Fregly BJ, Dimnet J (1998) Determination of joint functional axes from noisy marker data using the finite helical axis. Hum Mov Sci 17:1–15
- Clauser CE, McConville JT, Young JW (1969) Weight, volume, and center of mass of segments of the human body. Technical report AMRL-TR-69–70. Aerospace Medical Research Laboratory, Wright-Patterson Air Force Base, Dayton
- Davis RBI, Ounpuu S, Tyburski D, Gage JR (1991) A gait analysis data collection and reduction technique. Hum Mov Sci 10:575–587
- Dempster WT (1955) Space requirements for the seated operator. WADC technical report TR-55–159. Wright Air Development Center, Wright-Patterson Air Force Base, Dayton
- Doriot N, Chèze L (2004) A three-dimensional kinematic and dynamic study of the lower limb during the stance phase of gait using an homogeneous matrix approach. IEEE Trans Biomed Eng 51:21–27
- Dumas R, Chèze L, Verriest JP (2006) Adjustments to McConville et al. and Young et al. body segment inertial parameters. J Biomech (in press)

17. Dumas R, Nicol E, Chèze L (2006) Influence of perturbed gait data on four 3D inverse dynamic methods. In: Ninth symposium on 3D analysis of human movement, Valenciennes, France, 28–30 July: <http://www.univvalenciennes.fr/congres/3D2006/Abstracts/152-Dumas.pdf>
18. Dumas R, Aissaoui R, de Guise JA (2004) A 3D generic inverse dynamic method using wrench notation and quaternion algebra. *Comput Methods Biomech Biomed Eng* 7:159–166
19. Eng JJ, Winter DA (1995) Kinetic analysis of the lower limbs during walking: what information can be gained from a three-dimensional model? *J Biomech* 28:753–758
20. Gamage SS, Lasenby J (2002) New least squares solutions for estimating the average centre of rotation and the axis of rotation. *J Biomech* 35:87–93
21. Grood ES, Suntay WJ (1983) A joint coordinate system for the clinical description of three-dimensional motions: application to the knee. *J Biomech Eng* 105:136–144
22. Halvorsen K (2003) Bias compensated least squares estimate of the center of rotation. *J Biomech* 36:999–1008
23. Hartenberg RS, Denavit I (1964) Kinematic synthesis of linkages. McGraw-Hill, New York
24. Holden JP, Stanhope SJ (1998) The effect of variation in knee center location estimates on net knee joint moments. *Gait Posture* 7:1–6
25. Jalon JG, Bayo E (1994) Kinematic and dynamic simulation of mechanical systems—the real-time challenge. Springer, Heidelberg
26. Kadaba MP, Ramakrishnan HK, Wootten ME, Gainey J, Gorton G, Cochran GV (1989) Repeatability of kinematic, kinetic, and electromyographic data in normal adult gait. *J Orthop Res* 7:849–860
27. Kirtley C (2001) Summary: quaternions vs. Euler angles. *Biomch-L*: <http://www.isb.ri.ccf.org/biomch-l/archives/biomch-l-2001-05/00018.html>
28. de Leva P (1996) Adjustments to Zatsiorsky-Seluyanov's segment inertia parameters. *J Biomech* 29:1223–1230
29. Moio KC, Sumner DR, Shott S, Hurwitz DE (2003) Normalization of joint moments during gait: a comparison of two techniques. *J Biomech* 36:599–603
30. Most E, Axe J, Rubash H, Li G (2004) Sensitivity of the knee joint kinematics calculation to selection of flexion axes. *J Biomech* 37:1743–1748
31. Pearsall DJ, Costigan PA (1999) The effect of segment parameter error on gait analysis results. *Gait Posture* 9:173–183
32. Pearsall DJ, Reid JG (1994) The study of human body segment parameters in biomechanics. An historical review and current status report. *Sports Med* 18:126–140
33. Ramakrishnan HK, Kadaba MP, Wootten ME (1987) Lower extremity joint moments and ground reaction torque in adult gait. *Biomechanics of normal and prosthetic gait BED*. Am Soc Mach Eng 4:87–92
34. Rao G, Amarantini D, Berton E, Favier D (2005) Influence of body segments' parameters estimation models on inverse dynamics solutions during gait. *J Biomech* (in press)
35. Reid JG, Jensen RK (1990) Human body segment inertia parameters: a survey and status report. *Exerc Sport Sci Rev* 18:225–241
36. Reinbolt JA, Schutte JF, Fregly BJ, Koh BI, Haftka RT, George AD, Mitchell KH (2005) Determination of patient-specific multi-joint kinematic models through two-level optimization. *J Biomech* 38:621–626
37. Schache AG, Baker R (2006) On the expression of joint moments during gait. *Gait Posture* (in press)
38. Schwartz MH, Rozumalski A (2005) A new method for estimating joint parameters from motion data. *J Biomech* 38:107–116
39. Silva MP, Ambrosio JA (2002) Kinematic data consistency in the inverse dynamic analysis of biomechanical systems. *Multibody Syst Dyn* 8:219–239
40. Silva MP, Ambrosio JA (2004) Sensitivity of the results produced by the inverse dynamic analysis of a human stride to perturbed input data. *Gait Posture* 19:35–49
41. Spring KW (1986) Euler parameters and the use of quaternion algebra in the manipulation of finite rotations: a review. *Mech Mach Theory* 21:365–373
42. Stagni R, Leardini A, Cappozzo A, Grazia Benedetti M, Cappello A (2000) Effects of hip joint centre mislocation on gait analysis results. *J Biomech* 33:1479–1487
43. Vaughan CL, Davis BL, O'Connor JC (1992) Dynamics of human gait. Human Kinetics, Champaign
44. Woltring HJ, Huiskes R, de Lange A, Veldpaus FE (1985) Finite centroid and helical axis estimation from noisy landmark measurements in the study of human joint kinematics. *J Biomech* 18:379–389
45. Wu G, Cavanagh PR (1995) ISB recommendations for standardization in the reporting of kinematic data. *J Biomech* 28:1257–1261
46. Wu G, Siegler S, Allard P, Kirtley C, Leardini A, Rosenbaum D, Whittle M, D'Lima DD, Cristofolini L, Witte H, Schmid O, Stokes I (2002) ISB recommendation on definitions of joint coordinate system of various joints for the reporting of human joint motion—part I: ankle, hip, and spine. International Society of Biomechanics. *J Biomech* 35:543–548
47. Zatsiorsky VM, Seluyanov VN, Chugunova LG (1990) Methods of determining mass-inertial characteristics of human body segments. *Contemporary Problems of Biomechanics*: 272–291